

Coulomb Displacement Energies Derived from the (p,n) Isobaric Reaction*

J. D. ANDERSON, C. WONG, AND J. W. McCLURE

Lawrence Radiation Laboratory, University of California, Livermore, California

(Received 16 December 1964)

The agreement of Coulomb displacement energies derived from the nonmirror (p,n) isobaric reaction with those obtained from mirror and nonmirror ($T=1$) nuclei beta decay has been previously demonstrated. Using the Livermore 90-in. cyclotron time-of-flight facility, we have measured additional Coulomb displacement energies in the mass region $70 \leq A \leq 108$. These measurements indicate possible shell effects which were previously not observed because of the paucity of data. With the availability of 20.5-MeV protons, Coulomb displacement energy measurements were extended to the mass region $A \leq 165$. Even for nuclei as heavy as Ho¹⁶⁵, where the Coulomb displacement energy is 16.6 MeV, the width of the isobaric neutron group was not measurable (≤ 150 keV). The variation of the uniform radius parameter with atomic weight (A) inferred from these data is compared with that obtained from high-energy electron scattering experiments and is found to be in substantial agreement. A semiempirical formula for calculating Coulomb displacement energies is presented.

I. INTRODUCTION

THE agreement of Coulomb displacement energies derived from the (p,n) isobaric reaction^{1,2} and those obtained from mirror and nonmirror ($T=1$) nuclei beta decay^{3,4} has been previously demonstrated. The (p,n) measurements on nonmirror nuclei have not, however, shown the shell effects which are prominently displayed by the mirror nuclei data.³⁻⁵ The absence of these effects may have been due partly to the paucity of data.

Using the Livermore 90-in. cyclotron time-of-flight facility, we have measured additional Coulomb displacement energies in the mass region $70 \leq A \leq 108$. For a proton bombarding energy of 16.7 MeV, new measurements were made on targets of Ga and Sr, while for a bombarding energy of 18.4 MeV measurements were made for ³¹Ga, ³²Ge, ³³As, ³⁴Se, ³⁸Sr, ³⁹Y, ⁴⁰Zr, ⁴¹Nb, ⁴²Mo, ⁴⁵Rh, ⁴⁶Pd, and ⁴⁷Ag.

At 20.5-MeV bombarding energy, we have been able to extend the Coulomb displacement energy measurements into the region of the rare earths with measurements on targets of ⁵⁶Ba, ⁵⁸Ce, ⁵⁹Pr, ⁶⁰Nd, ⁶²Sm, ⁶⁴Gd, ⁶⁵Tb, and ⁶⁷Ho.

Using the Coulomb-energy calculation of Sengupta,⁶ a uniform radius parameter is obtained from the nonmirror (p,n) data and compared with that obtained from electron-scattering data.^{7,8} A semiempirical formula for calculating Coulomb displacement energies is presented which should be useful in identifying

isobaric states excited via other reactions.^{9,10} This formula should also be useful in shell-model calculations¹¹ when no direct measurement of the Coulomb displacement energy is available.

II. EXPERIMENTAL METHOD

The experimental geometry for the measurement of neutron spectra is essentially the same as previously reported (Ref. 1, Fig. 1). The neutron flight path varied from 8.9 to 11.7 m. The electronic system, including proton-electron pulse shape discrimination, has also been previously described.^{1,12} A larger stilbene crystal (2 in. in diam by 2 in. thick) is used to increase the neutron-detection efficiency.

Target thicknesses ranged from 100 to 200 keV. The Nb, Mo, Rh, and Ag were obtained commercially as foils. The Ge was evaporated on a $\frac{1}{4}$ -mil gold backing and the Se was evaporated on a $\frac{1}{2}$ -mil Mylar backing. The other targets, in the form of oxides, were prepared as colloidal suspensions with a $\frac{1}{2}$ -mil Mylar backing. All the targets are self-supporting in that the beam passes through them and the protons are collected in a shielded beam catcher.

III. RESULTS

The time-of-flight spectra resulting from 18.4-MeV proton bombardment of Ga and 20.0-MeV bombardment of Ce are shown in Fig. 1. The target gamma rays appear twice since a double display is used—one converter stop pulse for every two beam pulses.¹² The neutron groups correspond to; (A) configuration states,^{13,14} i.e., states in the residual nucleus having the same orbital configuration as the target nucleus but different isotopic spin ($\Delta T=1$), and (B) isobaric states

* Work performed under the auspices of the U. S. Atomic Energy Commission.

¹ J. D. Anderson, C. Wong, and J. W. McClure, Phys. Rev. **126**, 2170 (1962).

² J. D. Anderson, C. Wong, and J. W. McClure, Phys. Rev. **129**, 2718 (1963).

³ O. Kofoid-Hansen, Rev. Mod. Phys. **30**, 449 (1958).

⁴ J. Jänecke, Z. Physik **160**, 171 (1960).

⁵ J. H. Miller, III, Princeton University, thesis, Technical Report NYO-2959 (unpublished). J. H. Miller and D. C. Sutton, Bull. Am. Phys. Soc. **3**, 206 (1958).

⁶ S. Sengupta, Nucl. Phys. **21**, 542 (1960).

⁷ Beat Hahn, R. G. Ravenhall, and Robert Hofstadter, Phys. Rev. **101**, 1131 (1956).

⁸ R. Hofstadter, Ann. Rev. Nucl. Sci. **7**, 231 (1957).

⁹ J. L. Black and N. W. Tanner, Phys. Letters **11**, 135 (1964).

¹⁰ R. Sherr, M. E. Rickey, and C. G. Hoot, Bull. Am. Phys. Soc. **9**, 458 (1964).

¹¹ R. K. Bansal and J. B. French, Phys. Letters **11**, 145 (1964).

¹² J. D. Anderson and C. Wong, Nucl. Instr. Methods **15**, 178 (1962).

¹³ A. M. Lane and J. M. Soper, Nucl. Phys. **37**, 506 (1962).

¹⁴ Kiyomi Ikeda, Progr. Theoret. Phys. (Kyoto) **31**, 434 (1964).

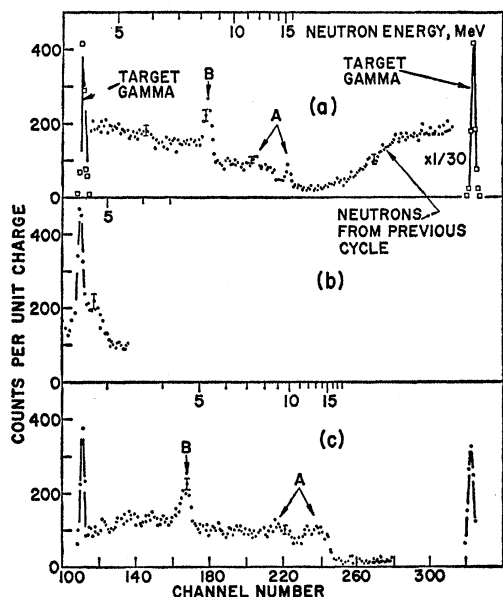


FIG. 1. Time-of-flight spectrum from 18.4-MeV proton bombardment of Ga (a) and 20.0-MeV proton bombardment of Ce (b) and (c). Time calibration of the system is 1.7 nsec/channel and increasing time-of-flight is toward the left. The flight paths were 11.39 m for Ga (a), 11.76 m for Ce (b), and 8.94 m for Ce (c). The prominent peaks are identified as follows; (A) configuration states ($\Delta T=1$), and (B) ($\Delta T=0$). The notation is that of Ref. 2.

($\Delta T=0$). From Fig. 1 one observes that the principal background obscuring the neutrons corresponding to the isobaric state is "boil-off" neutrons from compound-nucleus formation. The time-independent background (Fig. 1a, channel 235) is seen to be quite small. The target gamma rays are shown with (Fig. 1c) and without (Fig. 1a) proton-electron discrimination. The overlap of the target gamma ray and the isobaric neutron group (Fig. 1b) is removed (Fig. 1c) by varying the neutron flight path.

The energies of the neutrons are calculated from their time-of-flight¹⁵ while the energy of the incident protons is determined by means of a differential range measurement in aluminum. The isobaric (p,n) reaction Q values are summarized in Table I. The agreement with previous measurements^{1,2} is seen to be quite good. For many of the elements there are several isotopes, and the neutron peak is broadened due to different Coulomb energies for the various isotopes, e.g., for ${}_{62}\text{Sm}$ this broadening is about ± 150 keV. The centroid of the peak is used to calculate Q values quoted in Table I, and where a single isotope of an element is dominant ($>70\%$ abundance) its atomic weight is also listed. An over-all uncertainty of ± 150 keV is assigned to the Q value measurements. This error is about equally divided between the absolute uncertainty in the proton energy measurement and the reproducibility of the Q value measurements.

¹⁵ J. D. Anderson, C. Wong, and J. McClure, Nucl. Phys. **36**, 161 (1962).

TABLE I. Experimental Q values (Coulomb displacement energies) for the (p,n) isobaric reaction.^a

Target	Previous ^b	$\Delta E_c = \text{Iso}Q_{(p,n)}$ (MeV)			
		$E_p = 16.7$ MeV	18.4 MeV	20.0 MeV	20.5 MeV
Ar ⁴⁰	6.55 \pm 0.20				
Ti ⁴⁸	7.85 \pm 0.10		7.85		
V ⁵¹	8.05 \pm 0.10		8.15		
Cr ⁵²	8.40 \pm 0.15				
Fe ⁵⁶	8.85 \pm 0.15	8.9			
Co ⁵⁹	9.10 \pm 0.15				
Ni	9.45 \pm 0.13	9.5	9.5		
Cu ⁶³	9.55 \pm 0.12				
Cu ⁶⁵	9.40 \pm 0.12				
Zn	9.76 \pm 0.15				
Ga		10.3	10.1		
Ge	10.0 \pm 0.15	10.2	10.2		
As ⁷⁵				10.35	
Se	10.6 \pm 0.15	10.6	10.7		10.5
Sr ⁸⁸		11.6	11.45		
Y ⁸⁹	11.6 \pm 0.15		11.55		
Zr	11.75 \pm 0.15		11.75		
Nb ⁹³	11.95 \pm 0.15		11.95		12.0
Mo			12.0		
Rh ¹⁰³	12.8 \pm 0.15		12.8		12.9
Pd			13.0		
Ag	13.25 \pm 0.15		13.2		
In ¹¹⁵	13.5 \pm 0.2				
Sn	13.6 \pm 0.15			13.7	
Ba ¹³⁸				14.8	14.8
Ce ¹⁴⁰				15.4	15.2
Pr ¹⁴¹	15.4 \pm 0.25				
Nd				15.6	15.6
Sm				15.8	15.9
Gd				16.1	16.1
Tb ¹⁵⁹				16.5	16.3
Ho ¹⁶⁵				16.5	16.7

^a Where no error is indicated, assume ± 0.15 .

^b See Ref. 2.

For the rare earths, the energy width of the isobaric neutron group (~ 300 keV) is due to the target thickness (200 keV), the proton-beam energy spread (200 keV), the natural level width, plus an additional broadening when several isotopes are present. The natural level width for ${}_{67}\text{Ho}^{165}$ was not measurable in this experiment. Since the increase in width for ${}_{62}\text{Sm}$ (due to several isotopes) as compared to its monoisotopic neighbors (e.g., ${}_{67}\text{Ho}^{165}$) is measurable, we conclude that the natural level width of the isobaric counterpart of ${}_{67}\text{Ho}^{165}$ is ≤ 150 keV. This is in reasonable agreement with the calculations of Lane and Soper¹⁶ who predict no appreciable increase in level width as a function for A for $A > 80$.

IV. DISCUSSION

Coulomb Displacement Energies

Extensive use has been made of mirror-nuclei beta-decay energies to determine Coulomb displacement energies.^{3,4} For mirror nuclei the Coulomb displacement energy is identically the (p,n) Q value. For nonmirror nuclei the isobaric (p,n) reaction proceeds as follows: The incoming proton reacts with an "excess neutron"

¹⁶ A. M. Lane and J. M. Soper, Nucl. Phys. **37**, 663 (1962).

(a neutron corresponding to an unfilled proton state), exchanges its charge, and is emitted as a neutron. It is assumed that all the nuclear interactions within the initial and final nucleus are the same and thus the Q value for the (p,n) reaction leading to the isobaric state is the Coulomb displacement energy. The equivalence of the nuclear interactions has been discussed qualitatively by Ikeda *et al.*,¹⁷ more quantitatively by Pinkston,¹⁸ and is a natural consequence of the charge-independent optical-model formulation of Lane.^{19,20}

The Coulomb displacement energies derived from the (p,n) reaction on nonmirror nuclei are shown plotted in Fig. 2. The additional measurements around $A=90$ seem to indicate the presence of some shell effects. The relative errors on the data points are somewhat smaller than the 150-keV absolute errors which are shown. The measurements from Ba ($A=137$) to Ho ($A=165$) also tend to deviate from the average $Z/A^{1/3}$ dependence. It is clear from the rather large errors on the measurements that no quantitative remarks about shell effects on Coulomb displacement energies can be made.

Uniform Radius Parameter

To extract the uniform radius parameter from the Coulomb displacement energy we use the semiclassical expression of Sengupta.⁶ Assuming a uniform charge distribution within a sphere $R=r_0A^{1/3}$, he obtains

$$\Delta E_c(Z+1, Z) = [0.60(2Z+1) - 0.613Z^{1/3} - (-1)^Z 0.30](e^2/r_0A^{1/3}), \quad (1)$$

where Z is the charge of the nucleus, A is the atomic weight, r_0 is the uniform radius parameter, and e^2 is 1.440 MeV-F. The first term is the classical Coulomb

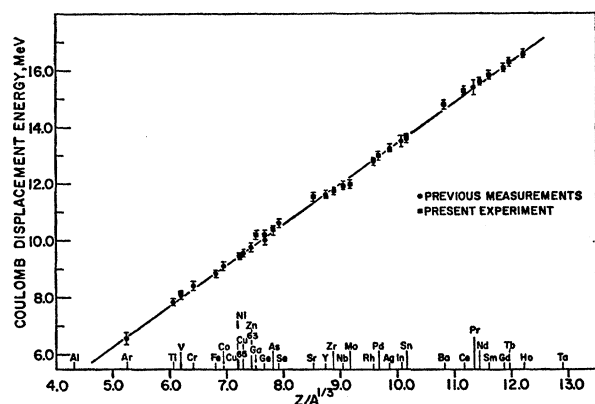


FIG. 2. The Coulomb displacement energies derived from the isobaric (p,n) reaction are plotted versus $Z/A^{1/3}$. The previous measurements are from Ref. 2.

¹⁷ K. Ikeda, S. Fujii, and J. I. Fujita, Phys. Letters 2, 169 (1962).

¹⁸ W. T. Pinkston (unpublished).

¹⁹ A. M. Lane, Phys. Rev. Letters 8, 171 (1962).

²⁰ A. M. Lane and J. M. Soper, Nucl. Phys. 35, 676 (1962).

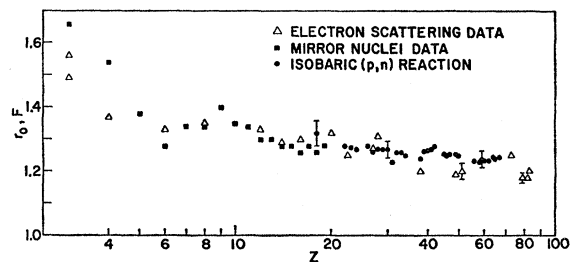


FIG. 3. The uniform radius parameter is plotted versus Z .

displacement energy while the second term comes from the exchange- and self-energy term in the Coulomb energy. The third term is a pairing term which is neglected for the (p,n) data since it is small compared to the error on the measurements.

In Fig. 3, r_0 is plotted versus Z . For Z less than 20 the values of r_0 are taken from Ref. 6, and for $Z > 20$ they are obtained from the present experiment. The uniform charge radii obtained from electron-scattering data^{7,8} are also shown. If one assumes that the only error in the radii derived from the present experiment is the uncertainty in the Q value measurements, then Δr_0 is approximately 1 to 2%. The errors on the electron-scattering results are comparable. The good agreement between the two sets of data may be fortuitous. It has been pointed out⁶ that neither the Coulomb-energy nor the electron-scattering results are uniquely determined by the root-mean-square radius of the charge distribution. Although the preceding comparison is consistent, i.e., a uniform charge distribution has been assumed throughout, a different assumption for the charge distribution may alter these results.

Semiempirical Results

Jänecke⁴ has described the Coulomb energy difference for $T=1/2$ and $T=1$ nuclei by a semiempirical expression as follows:

$$\Delta E_c(i \text{ shell}) = E_1(i)(\bar{Z}/A^{1/3}) + E_2(i) + \delta E_3 + \delta' E_4, \quad (2)$$

where \bar{Z} is the average charge, i.e.,

$$\bar{Z} = \frac{1}{2}(Z_{\text{initial}} + Z_{\text{final}}).$$

The coefficients E_1 and E_2 are shell-dependent while δE_3 and $\delta' E_4$ represent the difference in the Coulomb part of the proton pairing energy for the $T=1/2$ and $T=1$ nuclei, with

$$\begin{aligned} E_3 &= 0.120 \text{ MeV}, \\ E_4 &= 0.060 \text{ MeV}, \\ 2\delta &= 1 + (-1)^{\bar{Z}+1/2}, \\ \delta' &= +1 \text{ for } A=4n+2, T=1, T_Z=1 \leftrightarrow 0, \\ &= -1 \text{ for } A=4n+2, T=1, T_Z=0 \leftrightarrow -1, \\ &= 0 \text{ for } A \neq 4n+2. \end{aligned} \quad (3)$$

The expression $\delta E_3 + \delta' E_4$ takes on the values 0, 60,

and 120 keV. Since, as previously discussed, the shell effects which were so pronounced in mirror nuclei are barely discernible in the (p,n) data, and since the errors on the (p,n) data are larger than the proton pairing effects, it would seem reasonable for the (p,n) data to use the simple form:

$$\Delta E_c = E_1(\bar{Z}/A^{1/3}) + E_2. \quad (4)$$

The results of a weighted least-squares analysis of the (p,n) and mirror nuclei data are listed in Table II.

TABLE II. Coefficients of the semiempirical expression for the Coulomb displacement energy, $\Delta E_c = E_1\bar{Z}/A^{1/3} + E_2$, obtained from a least-squares analysis.

ΔE_c Data	E_1	E_2
(p,n)	1.443 ± 0.011	-1.12 ± 0.11
$T=1/2$	1.443 ± 0.026	-1.02 ± 0.12
All data [include $T=1/2$, $T=1$, and (p,n)]	1.436 ± 0.006	-1.05 ± 0.05
"Adjusted $T=1/2$ "	1.441 ± 0.018	-1.08 ± 0.08
All data [include "adjusted" $T=1/2$, $T=1$," and (p,n)]	1.444 ± 0.005	-1.13 ± 0.04

To circumvent the problems of shell and pairing effects, the mirror data were assigned an arbitrary error of 150 keV or the actual error on the measurement—which ever was larger. It is clear that a "best fit" to the (p,n) data agrees very well with the mirror nuclei data. The analysis revealed that for all cases the external error (based on the difference between the calculated and the observed value) was larger than the internal error (based on the assigned error on the measurement). The errors listed in Table II are based on the external error.

Since pairing effects are important for mirror nuclei the Coulomb pairing energies ($\delta E_3 + \delta' E_4$) were subtracted from the Coulomb displacement energies and the calculations were repeated with the "adjusted" data. Although there is little change in the coefficients of the least-squares fit to the data, the external error is reduced. The "adjusted" $T=1/2$ and $T=1$ data⁴ and the (p,n) isobaric reaction data from Table I are shown plotted in Fig. 4 along with the result of this least-squares analysis. From Fig. 4 it is seen that the largeness of the ratio of the external error to the internal error (~ 3) is not due to the presence of quadratic terms in the energy expression but is rather due to the large fluctuations of the data points around a "best" straight line. It is clear that for the mirror data the large external

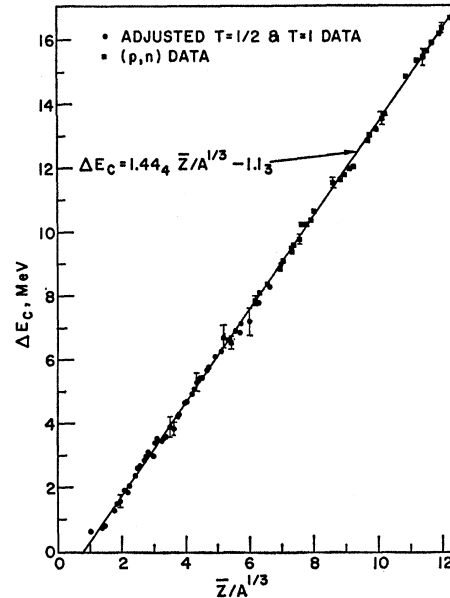


Fig. 4. The "adjusted" $T=1/2$, $T=1$ (see text) and the isobaric (p,n) Coulomb displacement energies are plotted versus $\bar{Z}/A^{1/3}$. A least-squares fit to the data is also shown. For the "adjusted" data, only errors larger than 150 keV are shown.

error is due to shell effects, and the large external error for the (p,n) data may indicate the presence of shell effects.

V. CONCLUSIONS

The Coulomb displacement energies from mirror nuclei data and those derived from the nonmirror (p,n) isobaric reaction are seen to be in excellent agreement. Although the (p,n) data analysis tends to indicate the presence of shell effects, the prominent shell effects displayed by mirror nuclei are surely reduced in the (p,n) process in that all neutrons corresponding to unfilled proton shells can contribute. The observation of isobaric states from proton capture reactions by Fox *et al.*^{21,22} and from the (p,d) reactions by Sherr *et al.*¹⁰ should in the future supply Coulomb displacement energy measurements that show a significant improvement in accuracy as well as being more amenable to a specific shell-model description.

²¹ J. D. Fox, C. F. Moore, and D. Robson, Phys. Rev. Letters **12**, 198 (1964).

²² J. D. Fox, D. D. Long, S. I. Hayakawa, and C. F. Moore, Bull. Am. Phys. Soc. **9**, 412 (1964).